











Simulating Quench Transients in the Self-Protected HL-LHC High Order Corrector Magnets

D. Mayr , L. Bender , E. Gautheron , S. Mariotto , M. Prioli , E. Ravaoli , M. Statera , E. Todesco ,
A. Verweij , and M. Wozniak 

Abstract—To meet the milestones set by the High-Luminosity LHC (HL-LHC) project, the integration of new inner triplet magnet circuits is vital for enhancing the focusing of the particle beams at ATLAS and CMS. In addition to the Nb₃Sn quadrupole magnets, high-order Nb-Ti magnets are required for field correction. This comprises self-protected magnets with six, eight, ten, and twelve poles, which also come in skewed variants. The simulation program LEDET was developed as part of the STEAM framework and is now applied to study quench transients in HL-LHC magnets. The electromagnetic and thermal transients occurring after a quench are simulated and validated with experiments at different current levels conducted by LASA (INFN). For the models, the three-dimensional geometry is accurately replicated and for each magnet the conductor parameters of each coil are set according to measurements. After discussing the various assumptions of the model, a simulation study is conducted to investigate the influence of the unknown quench location and inter-filament coupling losses. The developed models of each magnet show satisfactory accuracy and are predictive for different current levels. The models are then used to analyse the simulated hot-spot temperatures and peak voltages-to-ground, which cannot be easily measured. It is concluded that the protection strategy is effective.

Index Terms—Accelerator magnets, finite difference methods, modeling, Nb-Ti wire, quench protection, transient analysis.

I. INTRODUCTION

AS PART of the upgrade of the Large Hadron Collider to High Luminosity, the integrated luminosity (a measure of total number of collisions over a period of time) at the two main intersection points (ATLAS and CMS) will be increased by a factor of 5–7.5 to increase the statistical significance of physics experiments [1], [2]. This will require replacing the focusing inner triplet circuits [3].

Besides the Nb₃Sn quadrupole magnets that focus the beams, additional corrector magnets of higher harmonic order are

Manuscript received 26 September 2023; accepted 13 January 2024. Date of publication 26 January 2024; date of current version 20 February 2024. This work was supported by the High Luminosity LHC Project at CERN. (Corresponding author: D. Mayr.)

D. Mayr is with CERN, 1211 Geneva, Switzerland, and also with the Department of Mechatronics, University of Innsbruck, 6020 Innsbruck, Austria (e-mail: dany.mayr@gmail.com).

L. Bender is with badenovaNETZE, 79108 Freiburg, Germany.

E. Gautheron, E. Ravaoli, E. Todesco, A. Verweij, and M. Wozniak are with CERN, 1211 Geneva, Switzerland (e-mail: emm@cern.ch).

S. Mariotto, M. Prioli, and M. Statera are with the Laboratory of Acceleration and Applied Superconductivity, National Institute for Nuclear Physics (INFN), 20090 Milan, Italy.

Color versions of one or more figures in this article are available at <https://doi.org/10.1109/TASC.2024.3358772>.

Digital Object Identifier 10.1109/TASC.2024.3358772

TABLE I
KEY MAGNET AND CONDUCTOR DESIGN PARAMETERS

Parameter	MCSXF	MCOXF	MCDXF	MCTSXF	MCTXF
Magnet length	254 mm	233 mm	233 mm	200 mm	575 mm
Peak field	2.23 T	2.09 T	1.63 T	1.50 T	1.57 T
Op. temperature	1.9 K	1.9 K	1.9 K	1.9 K	1.9 K
Nom. current	99 A	102 A	92 A	84 A	85 A
Stored energy	1.72 kJ	1.55 kJ	0.67 kJ	0.73 kJ	3.63 kJ
Wire diameter	0.5 mm	0.5 mm	0.5 mm	0.5 mm	0.5 mm
Insul. thickness	70 μm	70 μm	70 μm	70 μm	70 μm
Cu/no-Cu ratio	2.1	2.1	2.1	2.1	2.1

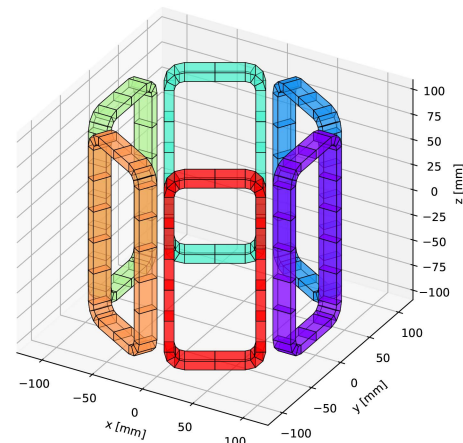


Fig. 1. Geometry of the symmetric racetrack coils of MCSXF approximated with hexahedrons. Created with STEAM-FiQuS.

needed to correct the magnetic field errors [4], [5], [6], [7], [8]. The sextupole (MCSXF) [9], [10], the octupole (MCOXF) [11], the decapole (MCDXF) [12] and the dodecapole (MCTXF) [13] magnets are designed to be self-protected. These magnets are also available as skewed variants, while all other parameters remain identical. Only the skewed variant of the dodecapole magnet (MCTSXF) deviates significantly from its counterpart, as its magnetic length is reduced to about one third. MCTSXF and MCTXF are therefore analyzed separately here. Table I gives an overview of the key design parameters of these Nb-Ti magnets designed and manufactured by LASA, INFN [14], [15]. The magnets are superferric, with racetrack coils exciting iron yokes that shape the magnetic field. As an example, the racetrack geometry for the MCSXF coils is shown in Fig 1.

It is expected that quenches may occur during the magnet operation. Local perturbations may lead to the transition of a small part of the superconductor to the normal conducting

TABLE II
OVERVIEW OF THE ANALYZED MEASUREMENTS

Magnet	Measurement No.	Current Level [A]	dI/dt [A/s]
MCSXF08	1 2	110.4 50.7	0.5 0.47
MCOXF05	3 4 5	73.6 82.3 100.7	0.5 0.5 0.43
MCOXF12	6	86.0	0.5
MCDXF11	7 8	101.6 111.1	-0.5 0.0
MCTSXF06	9	99.1	0.0
MCTXF04	10 11	41.0 96.0	0.5 0.38

state and most of the magnetic field energy is dissipated in the quenched part of the magnet. Low energy-density magnets can be designed to be self-protected, hence ensuring that the magnet stored energy is safely distributed in the coil windings without reaching excessive temperature or voltage-to-ground.

Each magnet test circuit includes a crowbar with a 6.8 m Ω resistor and a diode with a forward voltage of 0.85 V that are connected in parallel to the power-supply, thus providing a continuous path for the magnet current after the power-supply is switched off. This switch-off occurs when the voltage across the power-supply is higher than a predetermined threshold and assures that no additional energy is introduced into the circuit.

The STEAM framework [16] is used to model and simulate quench transients in superconducting accelerator magnets. The geometry input for the finite difference model is generated with STEAM-FiQuS [17], [18], [19], and the electromagnetic and thermal transients are simulated with STEAM-LEDET [20], [21]. The resulting models are validated with eleven quench events, collected during the magnet training campaign carried out at LISA, that occurred in different magnet types and at different currents. An overview of these measurement data are given in Table II.

With the validated models, the influence of the quench location is then investigated in a dedicated simulation study. In addition, the occurrence of quench back is investigated since coupling loss is modelled [22], [23], [24], [25]. Finally, hot-spot temperatures and peak voltages-to-ground are investigated for the conducted simulations and, in addition, also simulations at nominal conditions are performed and analyzed [26], [27].

II. MODELLING APPROACH

After the racetrack geometry is approximated as a hexahedron model (see Fig. 1), the coil hexahedrons are divided into the individual wire hexahedrons along the winding direction. The first and last wire hexahedrons of a coil are then connected according to the geometry of the used printed circuit board tracks. For each element, the magnetic field is then taken from experimentally validated three-dimensional (3D) OPERA simulations [4], [28], [29]. The 3D geometry and magnetic field is used as input for the LEDET program to simulate transients using a finite difference model. In Table III key parameters of the created models are listed, and in Fig. 2 the model of MCSXF with magnetic field is shown. For the simulation times a modern desktop computer was used to put this time into perspective. The number of time steps varies due to adaptive time stepping and different simulation time spans.

TABLE III
KEY PARAMETERS OF THE FINITE DIFFERENCE MODELS IN LEDET

Magnet Type	# Turns	# Nodes	# Time Steps	Simulation Time
MCSXF	1728	88977	600-700	\approx 40 min
MCOXF	2976	120849	700-800	\approx 100 min
MCDXF	2280	87385	600-700	\approx 90 min
MCTSXF	5328	142153	600-700	\approx 70 min
MCTXF	5328	544538	800-1000	\approx 240 min

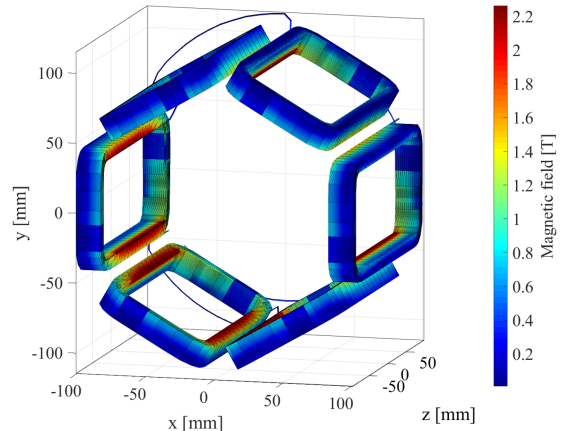


Fig. 2. Geometric representation of the finite difference model of MCSXF showing the initial magnetic field at the nominal current of 99 A.



Fig. 3. Picture of a scrapped MCTSXF cross-section showing single insulated wire in silver, epoxy in dark brown and coil insulation in light brown.

For each produced magnet, different conductor measurements were carried out for each coil. This allowed the conductor parameters RRR, Cu-to-Sc ratio, fitting parameters for the CUDI1 critical current function [30], filament-twist-pitch length to be adapted and applied in the models. The adjustment of these parameters can be carried out automatically in STEAM.

For the thermal modelling, the exact geometry and characteristics of all materials inside the magnet must be considered. The insulation thickness and wire diameter are known, but the amount of the epoxy between the insulated wires is difficult to determine, since its distribution is not homogeneous. In Fig. 3 this distribution can be seen in a cross-section of a MCTSXF coil. Since the epoxy is not distributed homogeneously, but rather occurs in pockets or at the edges, insulated wires are in good thermal contact. For this reason, it is a better approximation to neglect the thermal capacity of the epoxy between the wires rather than including it by assigning uniformly to all wires. To model the epoxy distribution more precisely, the exact wire positions and epoxy spread are essential. However, a single cross-sectional sample from a single magnet type does not offer universally applicable insights.

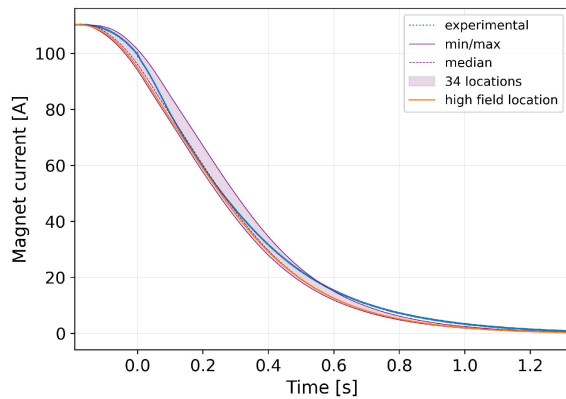


Fig. 4. Comparison of the measured current and the simulated one for 34 selected locations of quench origin in a MCSXF08 discharge at 110.4 A.

In LEDET, the power-supply could not be precisely modeled but only as an ideal current source. Using a workaround, the diode voltage U_d is applied from the start, which has a negligible effect on the simulation results.

Furthermore, the cooling is overestimated, since the model assumes that the wires on the four outer sides of each coil are in thermal contact with an ideal thermal sink at a constant temperature of 1.9 K. However, the coils are surrounded by liquid helium, which would require a more complex modeling of the cooling effect. To correct for this, a scaling factor f_c is introduced. To determine its optimum value, simulations are conducted for each measurement and the error in quench load is evaluated. The quench load, defined as the time integral of the square of the magnet current, affects the hot spot temperature under adiabatic conditions and is therefore often used as an easy to measure figure of merit for quench discharges. For this analysis, the quench location was set to the high-field region. It was shown that the error in quench load for the case $f_c = 0.1$ is the lowest, leading to a mean relative error of 7.5%. This parameter are therefore used for the final model.

III. MODEL VALIDATION

The last unknown is the quench location. Depending on the magnetic field, the number of adjacent conductors and the conductor parameters of each individual coil, the magnet discharge transient is slightly different. To take this into account in the model validation, the sensitivity of results to the uncertainty of the quench location was studied. For each magnet, the two coils with the highest and lowest resistance at 10 K were identified. Along the conductor each of these two coils, 17 locations uniformly distributed along the coil were selected. The number 17 was chosen because it has no common divisors/multiples with the number of turns in the height/width direction of the coils, and thus, no identical locations are simulated due to symmetries. As an example, the currents and resistive voltages simulated in these 34 cases for a quench at 100 A in an MCSXF magnet (measurement 4) are shown in Figs. 4 and 5, respectively. A band of minimum and maximum values, as well as their median, are plotted. The resistive voltage was not measured directly and is

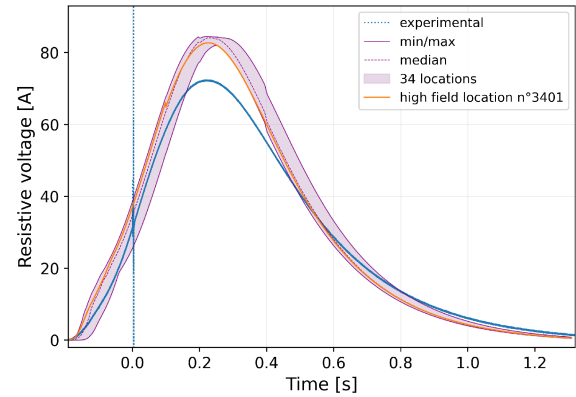


Fig. 5. Comparison of the measured resistive voltage and the simulated one for 34 selected locations of quench origin for a MCSXF08 discharge at 110.4 A.

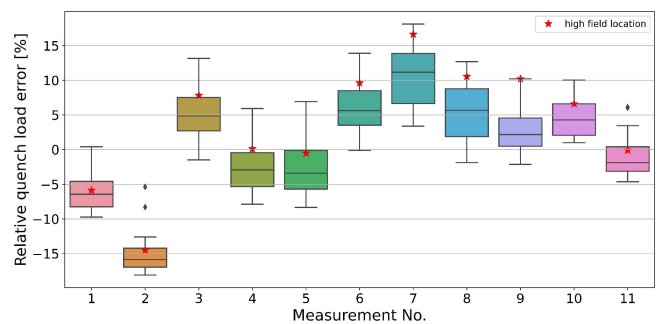


Fig. 6. Distribution of relative deviations in quench load from simulations with 34 selected quench locations and corresponding measurement.

calculated as the absolute difference of the voltage across the first and second half of the magnet windings.

Fig. 6 shows the relative quench load error for all quench locations and all measurements. It can be seen that the unknown quench location in the examined simulations introduces an uncertainty of about 9 to 16%. This varies from measurement to measurement, as different magnets have a wider range of conductor parameters and the selected locations can be placed in areas with different magnetic fields. It is, however, hard to determine in which of these locations a quench started in the analyzed test measurements. Only the simulation results for measurements 2, 7, and 10 are not within the uncertainty, as their error was never zero for the examined quench locations (see Fig. 6). Note that these are also measurements that are far from nominal conditions (see Table I and II).

At this point it should be mentioned, that by selecting only 17 equidistant quench locations in the coil, the locations resulting in fastest or slowest discharge may not be selected. Performing a larger number of simulations would improve the level of confidence in the simulations. However, the current level of model uncertainty estimation is deemed acceptable. In Fig. 6, magnet types show varied bias in quench load estimates. In particular, the first two measurements, which are conducted on MCSXF (see Table II), underestimate the quench load significantly with respect to other magnet types. The reason for this is probably that MCSXF has 32–40% more epoxy per half-turn with respect to the other magnets considered. Assuming epoxy neglect is

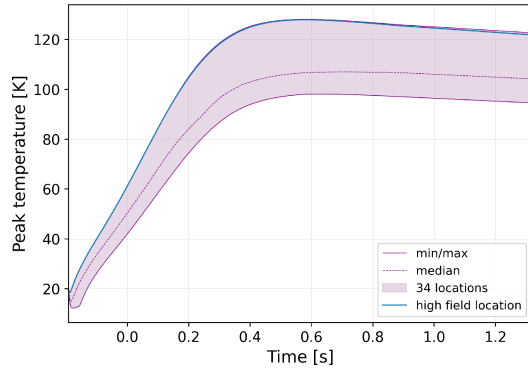


Fig. 7. Simulated hot-spot temperature course for 34 selected quench locations of MCSXF08 at 110.4 A (Measurement No. 1).

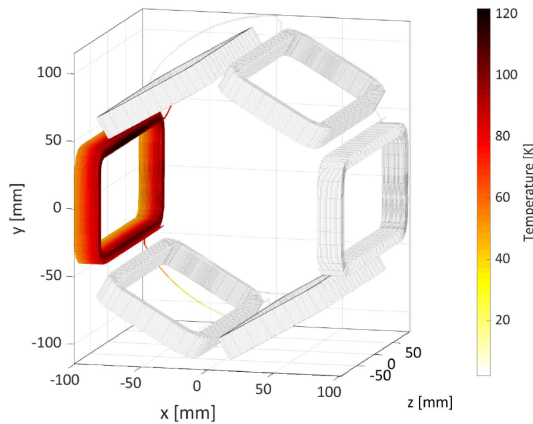


Fig. 8. 3D temperature distribution at the end of a MCSXF discharge at 110.4 A (Measurement No. 1) with quench starting in high-field location.

less ideal for MCSXF, but it is consistently more favorable than assuming a homogeneous distribution. To include the epoxy in the model, its distribution would need to be studied in more detail.

IV. SIMULATION RESULTS

A. Further Analysis of the Validation Simulations

After validating the magnet models against training measurement data, the simulated hot-spot temperatures and peak voltages-to-ground of these simulations are analyzed with regard to the magnet safety. In all conducted simulations and for all magnets, the hot-spot temperature remained below 130 K, and the voltages-to-ground never exceeded an absolute value of 150 V, thus maintaining safe thresholds. The minimum, maximum and median course of the simulated hot-spot temperatures obtained from the 34 simulations is shown for measurement 1 in Fig. 7. It can be seen that the unknown quench location introduces an uncertainty in the hot-spot temperature of about 30% and that the highest field location almost represents the worst case. The 3D temperature distribution at the end of this high-field quench location discharge in the left-side coil is shown in Fig. 8.

All validated simulation results are also used to assess whether interfilament coupling loss causes quench back in the magnet

TABLE IV
MAXIMUM SIMULATION RESULTS AT NOMINAL CONDITIONS

Magnet type	Hot-spot temperature	Peak voltage-to-ground
MCSXF	114 K	59 V
MCOXF	107 K	43 V
MCDXF	83 K	17 V
MCTSXF	81 K	21 V
MCTXF	103 K	103 V

coils. In none of the simulations, a quench was triggered in a coil different from the one initially quenching.

Moreover, simulations showed that the quench never propagated from the quenching coil to its electrical neighbors (see Fig. 8). Due to the limitations of the thermal model in the region of the coil connection wires, this should not be interpreted as a finding, but should be investigated further.

B. Simulations At Nominal Conditions

In addition, simulations in nominal conditions were carried out. Since the previous simulations showed a small deviation in hot-spot temperatures between the two selected coils with different conductor parameters (average relative difference is 1.8%, with a maximum of 4.9%), simulating only one coil is deemed sufficient for analyzing hot-spot temperatures.

However, peak voltages-to-ground are strongly affected by the quench location, and in particular the distance of the quenched coil to the electrical start/end of the magnet. In fact, a relatively high resistive voltage develops across the turns of the coil where the quench started, while the voltage across all other turns has opposite polarity. Thus, when the quench occurs in the first/last coil the large resistive voltage drop occurs close to the magnet ends, which are virtually to ground potential, and the peak voltage-to-ground is reached. On the contrary, when the quench occurs in other coils the resistive and inductive voltages partially compensate each other, and a lower peak voltage-to-ground is reached. For this reason, the previous analysis cannot be considered a worst case analysis for peak voltages-to-ground. For the simulation study at nominal conditions, 17 uniformly distributed locations are placed only in the electrically first coil.

The obtained hot-spot temperatures and peak voltages-to-ground in the worst selected case are shown in Table IV. All values are within an acceptable range. In various locations, the two parameters exhibit variations attributable to the differences in magnetic field strengths and the number of adjacent turn. Higher field intensities accelerate the quench propagation and the number of adjacent turns is influencing the transverse quench propagation.

V. CONCLUSION AND DISCUSSION

High order corrector magnets are needed for High Luminosity LHC to correct the magnetic field errors of the quadrupole magnets in the Inner Triplet circuits. These magnets comprise four different harmonic orders with different magnet parameters and geometries, and are designed to be self-protected. Electro-magnetic and thermal transients in these magnets were

simulated with STEAM-LEDET, which includes 3D thermal diffusion between turns, ohmic loss and inter-filament coupling loss. The 3D models rely on OPERA magnetic field calculations.

A single set of assumptions could be found that yielded simulations largely consistent with measurement data collected during training tests across all analyzed events for different magnets and operating conditions. The model accurately predicts quench discharge transients, aiding in performing LHC circuit simulations. The validated models are now part of the STEAM-models library.

The relative error in quench load for a high-field quench is within $\pm 17\%$ for all available measurements. By selecting and simulating 34 different quench locations for each magnet, it was shown that the unknown quench location plays a considerable role leading to a uncertainty of 9 to 16%.

The analysis showed the effectiveness of the self-protection strategy of the magnets, highlighting that at nominal conditions the simulated hot-spot temperatures and peak voltages-to-ground remain under 120 K and 110 V, respectively, across all magnet types and the selected quench locations. This reaffirms their readiness for deployment in the LHC.

REFERENCES

- [1] G. Apollinari, O. Brüning, and L. Rossi, "High luminosity LHC project description," CERN, Geneva, Switzerland, Tech. Rep. CERN-ACC-2014-0321, Dec. 2014. [Online]. Available: <https://cds.cern.ch/record/1974419>
- [2] G. Apollinari, I. Béjar Alonso, O. Brüning, M. Lamont, and L. Rossi, "High-luminosity large hadron collider (HL-LHC): Preliminary design report," CERN, Geneva, Switzerland, Tech. Rep. CERN-2015-005; FERMILAB-DESIGN-2015-02, 2015. [Online]. Available: <http://cds.cern.ch/record/2116337>
- [3] E. Todesco et al., "A first baseline for the magnets in the high luminosity LHC insertion regions," *IEEE Trans. Appl. Supercond.*, vol. 24, no. 3, Jun. 2014, Art. no. 4003305.
- [4] M. Statera et al., "Construction and power test of the superferric skew quadrupole for HL-LHC," *IEEE Trans. Appl. Supercond.*, vol. 30, no. 4, Jun. 2020, Art. no. 4003805.
- [5] M. Prioli et al., "Completion of the test phase for the hilumi LHC skew quadrupole corrector magnet," *IEEE Trans. Appl. Supercond.*, vol. 31, no. 5, Aug. 2021, Art. no. 4001205.
- [6] M. Statera et al., "Optimization of the high order correctors for HL-LHC toward the series production," *IEEE Trans. Appl. Supercond.*, vol. 31, no. 5, Aug. 2021, Art. no. 4002505.
- [7] M. Statera et al., "The HL-LHC high order correctors series production and powering tests status," *IEEE Trans. Appl. Supercond.*, vol. 32, no. 6, Sep. 2022, Art. no. 4004405.
- [8] E. Ravaoli et al., "Quench protection studies for the high luminosity LHC Nb₃Sn quadrupole magnets," *IEEE Trans. Appl. Supercond.*, vol. 31, no. 5, 2021, Art. no. 4700405.
- [9] G. Volpini et al., "Development of the superferric sextupole corrector magnet for the LHC luminosity upgrade," *IEEE Trans. Appl. Supercond.*, vol. 26, no. 4, Jun. 2016, Art. no. 4004804.
- [10] M. Statera et al., "Construction and cold test of the first superferric corrector magnet for the LHC luminosity upgrade," *IEEE Trans. Appl. Supercond.*, vol. 27, no. 4, Jun. 2017, Art. no. 4003205.
- [11] M. Statera et al., "Construction and cold test of the superferric octupole for the LHC luminosity upgrade," *IEEE Trans. Appl. Supercond.*, vol. 28, no. 4, Jun. 2018, Art. no. 4008705.
- [12] M. Statera et al., "Construction and cold test of the superferric decapole for the LHC luminosity upgrade," *IEEE Trans. Appl. Supercond.*, vol. 29, no. 5, Jun. 2018, Art. no. 4008705.
- [13] M. Sorbi et al., "Construction and cold test of the superferric dodecapole high order corrector for the LHC high luminosity upgrade," *IEEE Trans. Appl. Supercond.*, vol. 29, no. 5, Aug. 2019, Art. no. 4001905.
- [14] G. Volpini et al., "NbTi superferric corrector magnets for the LHC luminosity upgrade," *IEEE Trans. Appl. Supercond.*, vol. 25, no. 3, Jun. 2015, Art. no. 4002605.
- [15] M. Sorbi et al., "Status of the activity for the construction of the HL-LHC superconducting high order corrector magnets at LASA-Milan," *IEEE Trans. Appl. Supercond.*, vol. 28, no. 3, Apr. 2018, Art. no. 4100205.
- [16] "STEAM website," Accessed: Sep. 20, 2023. [Online]. Available: <https://espace.cern.ch/steam/>
- [17] "FiQuS website," Accessed: Sep. 20, 2023. [Online]. Available: <https://cern.ch/fiqus>
- [18] A. Vitrano, M. Wozniak, E. Schnaubelt, T. Mulder, E. Ravaoli, and A. Verweij, "An open-source finite element quench simulation tool for superconducting magnets," *IEEE Trans. Appl. Supercond.*, vol. 33, no. 5, Aug. 2023, Art. no. 4702006.
- [19] M. Wozniak, E. Ravaoli, and A. Verweij, "Fast quench propagation conductor for protecting canted cos-theta magnets," *IEEE Trans. Appl. Supercond.*, vol. 33, no. 5, Aug. 2023, Art. no. 4701705.
- [20] "LEDET website," Accessed: Sep. 20, 2023. [Online]. Available: <https://espace.cern.ch/steam/ledet>
- [21] E. Ravaoli, B. Auchmann, M. Maciejewski, H. Ten Kate, and A. Verweij, "Lumped-element dynamic electro-thermal model of a superconducting magnet," *Cryogenics*, vol. 80, pp. 346–356, 2016. [Online]. Available: <http://www.sciencedirect.com/science/article/pii/S0011227516300832>
- [22] G. H. Morgan, "Theoretical behavior of twisted multicore superconducting wire in a time-varying uniform magnetic field," *J. Appl. Phys.*, vol. 41, no. 9, pp. 3673–3679, 1970. [Online]. Available: <http://scitation.aip.org/content/aip/journal/jap/41/9/10.1063/1.1659491>
- [23] W. J. Carr Jr., "AC loss in a twisted filamentary superconducting wire. I," *J. Appl. Phys.*, vol. 45, no. 2, pp. 929–938, 1974. [Online]. Available: <http://scitation.aip.org/content/aip/journal/jap/45/2/10.1063/1.1663341>
- [24] A. P. Verweij, "Electrodynamics of superconducting cables in accelerator magnets," Ph.D. dissertation, Twente Univ., Enschede, The Netherlands, 1995. [Online]. Available: <https://cds.cern.ch/record/292595>
- [25] E. Ravaoli et al., "Modeling of inter-filament coupling currents and their effect on magnet quench protection," *IEEE Trans. Appl. Supercond.*, vol. 27, no. 4, Jun. 2018, Art. no. 4000508.
- [26] M. Mentinik, "Report: Cross-check of protection studies of the HL-LHC high order corrector magnets." Jun. 8, 2020. Accessed: Sep. 20, 2023. [Online]. Available: <https://edms.cern.ch/document/2222750/1.3>
- [27] M. Prioli and S. Mariotto, "Engineering specification: Quench protection study for the hi-luminosity LHC HICH order corrector magnets," Apr. 28, 2020. Accessed: Sep. 20, 2023. [Online]. Available: <https://edms.cern.ch/document/2370274/1>
- [28] L. Fiscarelli et al., "Magnetic measurements on the prototype magnets of the high-order correctors for HL-LHC," *IEEE Trans. Appl. Supercond.*, vol. 29, no. 5, Aug. 2019, Art. no. 4003505.
- [29] E. De Matteis et al., "Magnetic measurements results and analysis of the first batches of superferric magnets for the HL-LHC high order field correction," *IEEE Trans. Appl. Supercond.*, vol. 32, no. 6, Sep. 2022, Art. no. 4004905.
- [30] A. Verweij, *CUDI: Users Manual*, CERN, Geneva, Switzerland, 2007.